# Numerical Human Head Model for Traumatic Injury Assessment

**Hyung-Yun Choi***
*Department of Mechanical and System Design Engineering, Hong-Ik University, Seoul 121-791, Korea*

The finite element human head model is developed for traumatic injury assessment. The model is constructed based on the precise anatomical geometry and validated with test results. In this paper, structural and physiologic explanation of human head will be introduced as well as the modeling methodology. Some of simulation results are also chosen to present major features of the model.

**Key Words** : Finite Element Human Head Model, Traumatic Injury

## 1. Introduction

The finite element model of human head has been developed in order to study the basic injury mechanisms due to the dynamics loading such as crash. The human head-neck complex is well exposed to the abrupt translational and rotational movement compared to the rest of body parts during the crash accident. These kinds of movement often cause serious injuries of head-neck complex even without direct contact with the foreign objects. Relative movement of brain inside the skull, mainly caused by its inertia, would cause vascular injury on the connecting vessels and also may induce a negative pressure in subarachnoidal space, which result in axonal injuries. These understanding of basic injury mechanisms of human head-neck complex, however, are quite limited to some extent and many studies are under going both experimentally (Nahum, 1977; Bandak, 1996; Donnelly, 1997) and analytically (Claessens, 1997; Willinger, 1999; Ruan, 1993; Zhou, 1995; Zhou, 1994; Bandak, 1994; Kim, 1998; Voo, 1996). Recently numerical simulations, especially using the finite element method, have been utilized to investigate the hypothetical theories based on experiments and clinical findings. Quite many numbers of finite element human head models had been developed for this purpose and evolutions of computational models have been remarkable thanks to the advance of computational powers and the FE codes. The one of the distinguishing feature of head model in this study would be the precise modeling of the fluid-solid interactions. The structural role of cerebrospinal fluid (CSF) occupying the subarachroidal space in the brain is cushioning and buffering between the skull and brain as well as transmitting the forces. The Murnaghan equation of state for solid element has been employed to model the CSF layers in head and dura sec of cervical spinal foramen. The incompressible behavior of CSF in the head, which has the closed volume, also induces a "cavitation" when the brain has sufficient relative motions inside the skull. The ideal gas equation is, thus, applied in order to simulate this cavitational phenomenon. These newly attempts in the head model produce more realistic results than the previous head models do.

* Corresponding Author,
**E-mail** : hychoi@wow.hongik.ac.kr
**TEL** : +82-2-320-1699 ; **FAX** : +82-2-326-0368
Department of Mechanical and System Design Engineering, Hong-Ik University, 72-1 Sangsu-dong, Mapo-gu, Seoul 121-791, Korea.

## 2. Anatomy of Human Head and Typical Injury Pattern Due to the Dynamic Loading

### 2.1 Cranial structure

The skull consists of three layers referred to as

the outer table, diploe, and inner table. The diploe consists of trabecular bone, and is located between the other two that are made up of compact bone. This arrangement exhibits great variability in the relative thickness of the layers. The inside surface of the cranial cavity is lined by a layer of dense fibrous irregular connective tissue and enclosing venous sinuses. This layer adheres for the most part tightly to the cranial bones.

### 2.2 Intracranial structure

The intracranial structure contains mainly the brain, cerebrospinal fluid, vascular structure, and the membranous coverings and partition structures. The cerebrum occupies most of the cranium and is composed of right and left hemispheres separated by a folding extension of the dura mater called the falx cerebri. The cerebrum and the cerebellum are separated by another fold of the dura mater called the tentorium cerebelli. The junction between the folds of the dura and the inner surface of the cranium forms some of the venous sinuses. The next layer below the dura mater is the arachnoid. This is a delicate avascular membrane having a spider web arrangement of delicate collagen fibers that surrounds the brain and envelopes the outer surface of the brain. It is bounded from above by the subdural space and from below by the pia mater. The pia mater is a thin transparent connective tissue layer that adheres to the surface of the brain and the spinal cord. It consists of interlacing bundles of collagen fibers and some fine elastic fibers and contains many blood vessels. It also continues as a sheath around the many small vessels that penetrate into the brain. The space between the arachnoid and the pia mater is called the subarachnoidal space which is traversed by the arteries of the brain and cranial nerves and contains cerebrospinal fluid. The cerebrospinal fluid (CSF) continuously circulates through the subarachnoid space around the brain and spinal cord and through cavities within the brain. These are four cavities called ventricles; two lateral ventricles, one in each of the cerebral hemispheres; the third ventricle is a vertical slit at the mid-line below the lateral ventricles and the right and left halves of the thalamus, with the thalamus forming the lateral walls of the third ventricle; and the fourth ventricle lies between the brain stem and the cerebellum.

Major head injuries are skull fractures and brain damages. Most of skull fractures are from direct impact with foreign object on head and brain damage, on the other hand, is from secondary impact within the cranial space and/or relative motions between skull and brain. Brain injury is often classified into diffuse and focal injuries according to their causes and symptoms.

## 3. Numerical Modeling of Human Head-Neck Complex

The volumetric geometries of the head components were extracted from the Visible Human data set (http://www.nlm.nih.gov/research/visible/visible human.html; Choi, 1999). Figure 1 shows the process of constructing the head model. Material properties assigned to bony components, brain matter and soft tissues in the model are

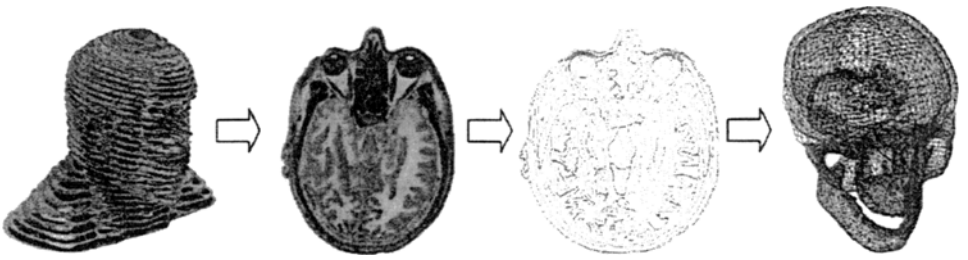


**Fig. 1** Process of digitization and building the finite element model of human head (1; Visible Human; 2; Transverse section, 3; Digitized section, 4; Meshed human head)

**Table 1** Mechanical properties of head model

| Component | | $E$ | $B$ | $G$ | $\nu$ | $\rho$ |
|---|---|---|---|---|---|---|
| Skull | Outer table | $7.3\times10^6$ | | | 0.22 | 3000 |
| | Inner table | $7.3\times10^6$ | | | 0.22 | 3000 |
| | Diploe | | $2.02\times10^5$ | $1.39\times10^5$ | 0.22 | 1410 |
| Facial bone | | $7.3\times10^6$ | | | 0.22 | 2700 |
| Mandible | | $7.3\times10^6$ | | | 0.22 | 2700 |
| Dura mater | | $3.15\times10^4$ | | | 0.22 | 1133 |
| Venous sinus | | | $1.0\times10^5$ | | | 1000 |
| CSF | | | $1.0\times10^5$ | | | 1000 |
| Falx | | $3.15\times10^4$ | | | 0.45 | 1133 |
| Pia | | $3.15\times10^4$ | | | 0.45 | 1133 |
| Tentorium | | $3.15\times10^4$ | | | 0.45 | 1133 |
| Brain | Gray matter | | $7.96\times10^3$ | $7.96\times10^1$ | 0.499 | 1040 |
| | White matter | | $1.27\times10^4$ | $1.27\times10^2$ | 0.499 | 1040 |
| Ventricle | | | $1.0\times10^5$ | | | 1000 |
| Cerebellum and stem | | | $1.27\times10^4$ | $1.27\times10^2$ | 0.499 | 1040 |

E=Young's modulus (KPa), B=Bulk modulus (KPa), G=Shear modulus (KPa),
$\nu$=Poisson s ratio, $\rho$=Mass density (kg/m$^3$),

acquired from various published open literatures listed in Table 1. Brain matters, grey and white, were modeled as linear visco-elastic materials based on in-vitro shear modulus measurement (Donnelly, 1997).

## 4. Case Studies: Selected Simulation Results

### 4.1 Frontal pendulum impact simulation

The experimental study using the cadavers performed by Nahum et al. (1977) was used to validate the head model for the case of linear acceleration loading. Since the neck was excluded in this simulation, a free-boundary condition was applied to the head-neck joint. This constraint is justified by the findings of Willinger et al. (1999) and Ruan et al. (1993) who showed that the neck does not influence the kinematic head response during the pulse duration. The impact was delivered by a pendulum along the axis inclined at about 45° to the Frankfort plane in mid-sagittal plane (Fig. 2). The mass and initial velocity of the pendulum were 6 kg and 5.9 m/s, respectively. Model responses were compared with the measured cadaver test data in terms of impact force, head acceleration (CG), and epidural pressures.

As expected, we could observe the relative motion between the brain and the dura, posterior cavity, and flow of the CSF layer. The comparisons of the numerical and experimental forces and head accelerations are shown in Fig. 3. The calculated impact force showed a good correlation with Nahum's test, but the head acceleration did not match well due to the small difference in head mass.

The precedent models have measured the intracranial pressures at the selected brain element. On the other hand, the measured locations of pressure histories reported in Nahum's tests are the subarachnoidal space between skull and brain. Figure 4 present the calculated pressures at various region compared with Nahum's tests (1977) and Willinger's simulation (1999). Calculated pressure levels in both brain elements and subarachnoidal

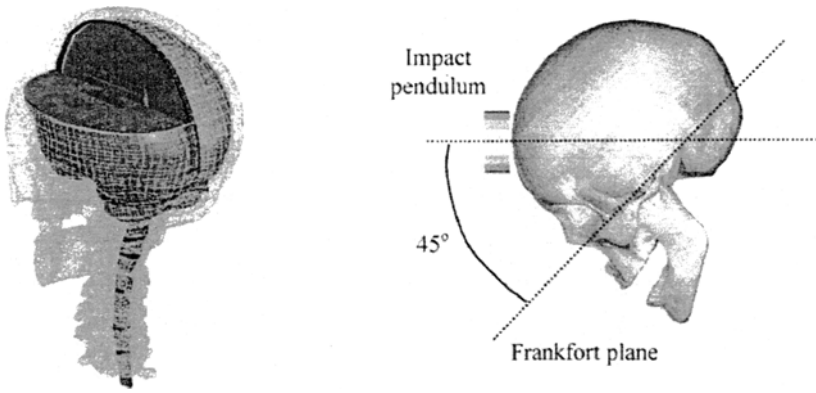


**Fig. 2** Finite element head model and impact condition

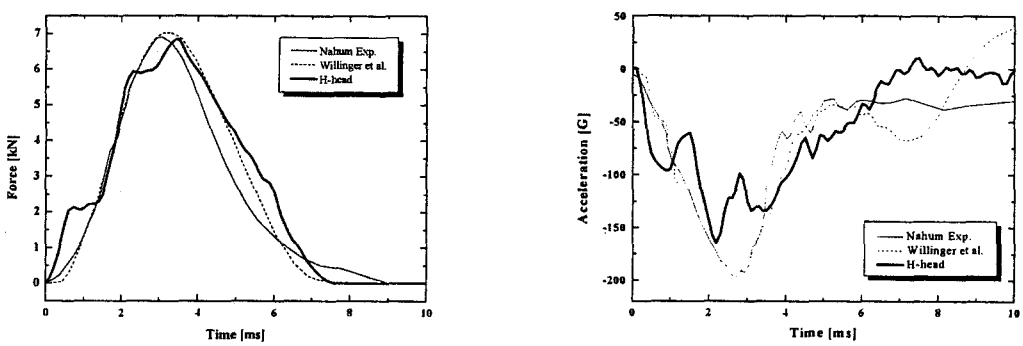


**Fig. 3** Comparisons of impact force (left) and COG acceleration (right) between simulation and test

space are shown in the figures for the qualitative comparisons with the test and other simulation results. The general trends of pressure histories from the calculation and test correlate quite well considering the possible geometric discrepancies between model and specific cadaver specimen. High positive peak pressures appeared beneath the impact site in the frontal region and the greatest negative pressures were generated at the posterior fossa which, due to the inclination of the skull, was the area opposite the impact site. The coup-contrecoup pressures were considerably asymmetric. The head model predicted a maximum pressure of 250 kPa in the frontal region and a minimum pressure of -40 kPa in the contrecoup region. It is remarkable that the trends of the pressure distribution were somewhat different along the measuring locations. Overall, the reference data are positioned on the pressure curves between the brain surface and the vacuum cavity. The reason why various patterns of pressure at this space appear is that some materials having quite different properties exist between the brain and the dura mater. Figure 5 shows the movement of head components and the pressure contour of the brain surface. The pressure gradients changed smoothly from the frontal to the posterior regions and a higher negative pressure, which representing a probability of cavitation, occurred at the occipital and posterior area. At the end of the acceleration period, the contrecoup pressure shows a rapid pressure increase of about 30 kPa within a few milliseconds. This rapid increase could be the result of cavitation bubble collapse. Following the acceleration, the coup side pressure continues to drop below zero, which is an indication that cavitation has also occurred at the coup side. The origin of the cavitation cannot be determined with certainty, but it is plausible that it arises from the flow that occurs from the coup to contrecoup as a result of the initial acceleration. When the acceleration pro-

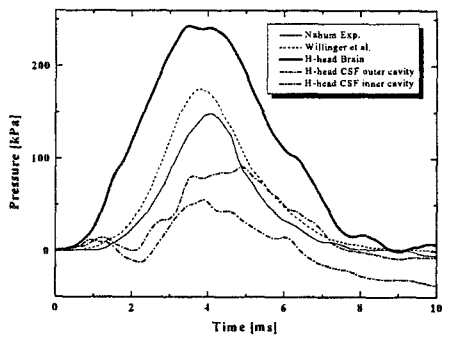


(a) Frontal pressure (coup pressure)

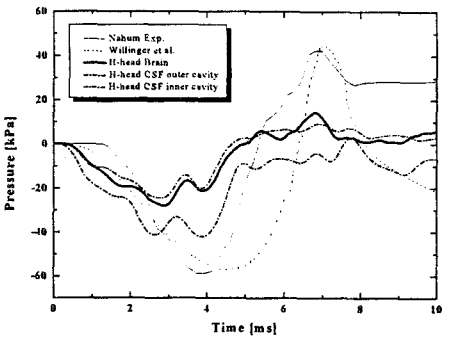


(b) Posterior pressure (contrecoup pressure)

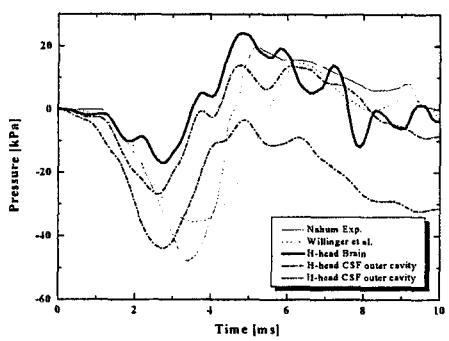


(c) Occipital pressure

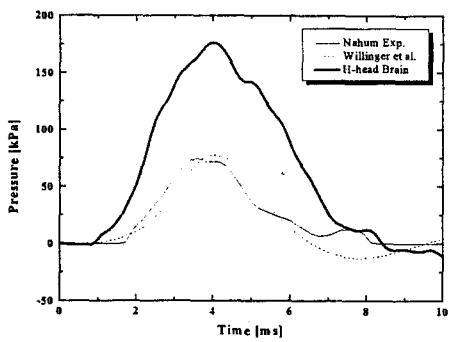


(d) Parietal pressure

**Fig. 4** Comparisons of brain pressures between simulation and test

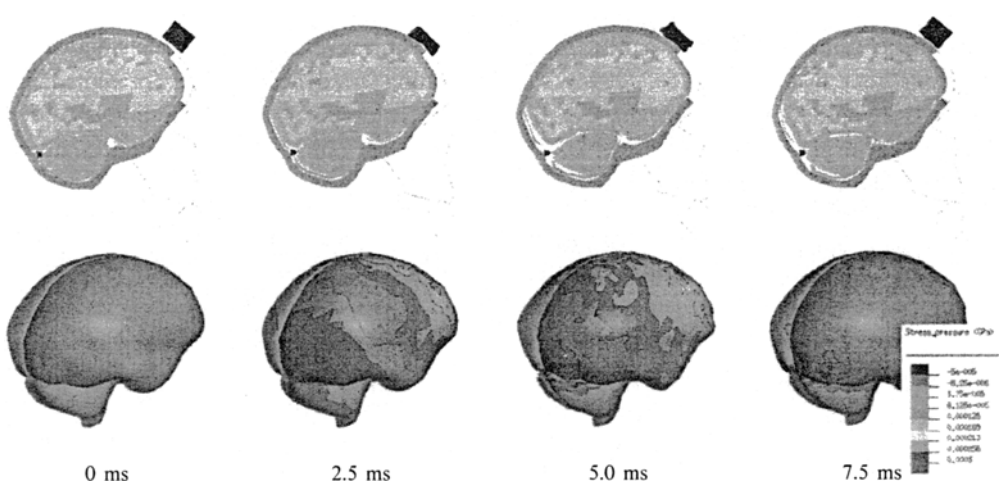


**Fig. 5** Sectional view and pressure distributions on brain

duces cavitation, the character of the pressure variation changes dramatically. These results suggest that there is a critical acceleration at which cavitation and its subsequent damage appear.

### 4.2 Combined acceleration simulation

Analytical simulation of diffuse axonal injury was carried out using the head model. The loading was applied to the skull by imposing an angular velocity about an axis passing through a point 30.48 cm below the center of gravity (Fig.

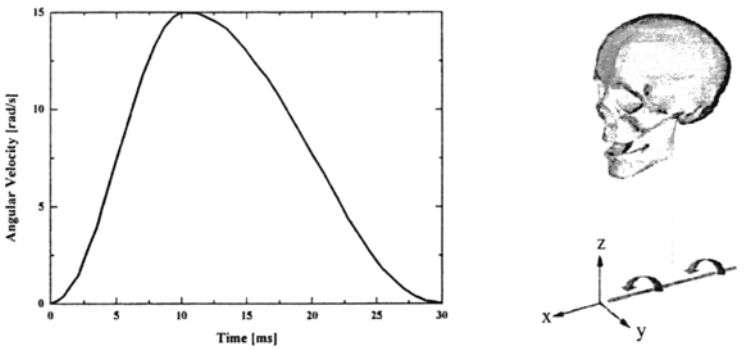


**Fig. 6** Loading condition for combined acceleration

(a) $\gamma_{xy}$ (b) $\gamma_{yz}$ (c) $\gamma_{zx}$

**Fig. 7** Shear strain distribution for sagittal and transverse section (t=10.5 ms)

6). Combined rotational and translational acceleration that might be expected under automotive crash were produced in medial-lateral plane. The rotational velocity-time histories was taken from the simulations done by Bandak et al. (1994).

Since it was hypothesized that localized and concentrated shear strain is a major cause of DAI, it would be reasonable to compare the patterns of shear strain distributions calculated by head model with the sites of DAI in other references (Zhou, 1994; Bandak, 1994; Kim, 1998). Shear strain distributions are shown in Fig. 7. Although the head model does not have fine geometry of the corpus callosum which is located very center of the brain and has somewhat fibrous composition resulting in brittle behavior in deformation, contour of the shear strain in yz components shows quite concentrated patterns at the center of the brain. These shear strain patterns correspond well with the typical locations of DAI. DAI tends to occur in the white matter at its border with the gray matter and around the ventricles suggesting that shear strain is a possible cause for the development of DAI.

## 5. Conclusion

The objectives of finite element human model including head-neck model presented in this paper for occupant safety simulation is to understand basic injury mechanism and quantitatively assess the injury levels due to the dynamic loading. By applying the precise anatomic structures and material properties of each body components, constructed finite element model could simulate deformational behavior of human body similar to the real event. In order to utilize these FE models and simulation results to predict the detail injury levels, further validation procedure is needed.

## References

Bandak, F. A. and Eppinger, R. H. , 1994, "A Three-Dimensional Finite Element Analysis of the Human Brain Under Combined Rotational and Translational Accelerations," SAE 942215, pp. 145~163

Bandak, F. A., 1996, "Biomechanics of Impact

Traumatic Brain Injury," *Proceedings of the NATO-ASI on Crashworthiness of Transportation Systems*, pp. 213~253.

Choi, H. Y., Lee, I. H. and Haug, E., 1999, "Advanced Finite Element Modeling of the Human Body for Occupant Safety; H-Model for the Next Millennium" *Proceeding of 5th HanPam*, p. 295.

Claessens, M., Sauren, F. and Wismans, J., 1997, "Modeling of the Human Head Under Impact Conditions: A Parametric Study," *Proceedings of the 41st Stapp Car Crash Conference*, pp. 315~328.

Donnelly, B. R. and Medige, J., 1997, "Shear Properties of Human Brain Tissue," *Journal of Biomechanical Engineering*, Vol. 119. pp. 423~432.

Kim Y. E. and Nam D. H., 1998, "Analysis of the Diffuse Axonal Injury of the Human Brain using Finite Element Model," *J. of KOSOMBE*. Vol. 19, pp. 603~609.

Nahum, A. M., Smith, R. and Ward, C. C., 1977, "Intracranial Pressure Dynamics During Head Impact," *Proceedings of the 21st Stapp Car Crash Conference*, pp. 339~366.

Ruan, J. S., Khalil, T. B. and King, A. I., 1993, "Finite Element Modeling of Direct Head Impact," *Proceedings of the 37th Stapp Car Crash Conference*, pp. 69~81.

Visible Human Project, http://www.nlm.nih.gov/research/visible/visible human.html

Voo, L., Kumaresan, S., Pintar, F. A., Yoganandan, N. and Sances, A., Jr, 1996, "Finite-Element Models of the Human Head," *Medical & Biological Eng. & Computing*, pp. 375~381.

Willinger, R., Kang, H. S. and Diaw, B., 1999, "Three-Dimensional Human Finite-Element Model Validation Against Two Experimental Impacts," *Annals of Biomedical Eng*. Vol. 27, pp. 403~410.

Zhou, C., Khalil, T. B., King, A. I. and 1994, "Shear Stress Distribution in the Porcine Brain Due to Rotational Impact," *Proceedings of the 38th Stapp Car Crash Conference*, pp. 133~143.

Zhou, C., Khalil, T. B. and King, A. I., 1995, "A New Model Comparing Impact Responses of the Homogeneous and Inhomogeneous Human Brain," *Proceedings of the 39th Stapp Car Crash Conference*, pp. 121~137.